Forward-backward multiplicity and momentum correlations in *pp* and *p*Pb collisions at the LHC energies

Joyati Mondal,[1,*] Hirak Koley,[1] Somnath Kar,[2,1,†] Premomoy Ghosh,[1] Argha Deb,[1,3] and Mitali Mondal[1,3,‡]

[1]*Department of Physics, Nuclear and Particle Physics Research Centre, Jadavpur University, Kolkata—700032, India*

[2]*University Department of Physics, Kolhan University, Chaibasa—833201, India*

[3]*School of Studies in Environmental Radiation and Archaeological Sciences, Jadavpur University, Kolkata—700032, India*

(Received 6 January 2023; accepted 11 May 2023; published 13 June 2023)

Correlations and fluctuations between produced particles in an ultrarelativistic nuclear collisions remain one of the key observables to understand the fundamentals of the particle production mechanism. More differential tools like forward-backward (FB) correlations between particles from two different phase spaces further strengthened our understanding. We study the strength of FB correlations in terms of charged-particle multiplicity and summed transverse momentum for proton-proton (pp) and proton-lead (pPb) collisions at center-of-mass energies $\sqrt{s} = 13$ TeV and $\sqrt{s_{\rm NN}} = 5.02$ TeV, respectively, for the EPOS3 simulated events with hydrodynamical evolution of produced particles. Furthermore, the correlation strengths are separately obtained for the particles coming from the core and the corona. FB correlation strengths are examined as a function of the pseudorapidity gap ($\eta_{\rm gap}$), pseudorapidity window width ($\delta\eta$), center-of-mass energy ($\sqrt{s}$), minimum transverse momentum ($p_{T_{\rm min}}$), and different multiplicity classes following standard kinematical cuts used by the ALICE and ATLAS experiments at the LHC for all three EPOS3 event samples. The EPOS3 model shows a similar trend of FB multiplicity and momentum correlation strengths for both pp and pPb systems, though the correlation strengths are found to be larger for the pPb system than for the pp system. Moreover, the $\delta\eta$-weighted average of FB correlation strengths as a function of different center-of-mass energies for pp collisions delineates a tendency of saturation at very high energies.

DOI: 10.1103/PhysRevD.107.114016

I. INTRODUCTION

The formation of a hot dense medium of quasifree quarks and gluons, known as the quark-gluon plasma (QGP), in relativistic heavy-ion collisions at the Relativistic Heavy Ion Collider (RHIC) and the Large Hadron Collider (LHC) provides a unique opportunity to explore the early Universe and validate the theory of strong interactions between quarks mediated by gluons [1–3]. The relativistic viscous hydrodynamic calculations [4,5] have been found to be most successful in explaining the properties of the produced hot and dense matter in heavy-ion collisions and demonstrate the space-time evolution of the medium through observables such as harmonic flow (v_n) [6–8], which represent the translation of initial-state spatial inhomogeneities to the final-state momentum anisotropies.

In heavy-ion collisions, the initial energy density fluctuates strongly event to event which leads to the fluctuations of the space-time evolution of the produced medium in the final state. Owing to the viscous hydrodynamics, such density fluctuations are manifested as anisotropic harmonic flow. The large initial-state fluctuations effectuate the observed long-range correlations (LRCs) between final-state particles which are observed as a correlation between multiplicity densities in different pseudorapidity (η)-windows [9]. Another aspect of longitudinal multiplicity correlations is the short-range correlations (SRCs) localized over a smaller range of η, manifested in the single jet, minijets, resonance decays, etc. Forward-backward (FB) correlations between charged-particle multiplicities or transverse momenta in two symmetrically separated η-windows about the collision vertex motivate us to differentiate between LRC and SRC components [10] and to study the dynamics of the particle production mechanism in high-energy hadron or nuclear collisions.

Positive FB multiplicity correlation strength was first observed in $p\bar{p}$ collisions at $\sqrt{s} = 540$ GeV at the CERN

*joyati254@gmail.com
†somnathkar11@gmail.com
‡mitalimon@gmail.com

SPS collider [11], and it has been then rigorously inspected in $p\bar{p}$ collisions at the Intersecting Storage Rings (ISR) energies from $\sqrt{s} = 200$ to 900 GeV [12,13]. Later, FB correlations were also examined in pp and $p\bar{p}$ collisions over a wider range of collision energies [14–16]. No significant FB multiplicity correlation has been reported in e^+e^- collisions [17], whereas a very weak correlation strength was observed in e^+e^- annihilation [18,19]. The clan structure has been used for better understanding of observed stronger positive FB correlation in pp and $p\bar{p}$ collisions compared to weak correlation in e^+e^- annihilation [20]. There are also significant positive FB correlation values reported in different collision systems, e.g., pp, pA, and AA collisions [9,21–24]. The ATLAS [23] and ALICE [24] Collaborations at the LHC reported strong FB correlations in pp collisions at $\sqrt{s} = 0.9$, 2.76, and 7 TeV, which contradicts STAR Collaboration's findings of weak correlation [22].

To explain the experimental results, numerous theoretical models have been put forth. In the dual parton model (DPM) [25], a Pomeron exchange between colliding hadrons was initially thought of as an inelastic scattering; later, the idea of many Pomeron exchanges was implemented. The DPM projected that particles created in two well-selected rapidity intervals would have a significant long-range correlation [26]. The quark gluon string model (QGSM) [27,28] is similar to the DPM with some essential differences. In this model, new objects—quark-gluon strings—are formed which fragment into hadrons and resonances. The QGSM model successfully described ALICE data and concluded that the multistring processes due to multi-Pomeron exchanges were the main contributor to the FB correlations. The string fusion model (SFM) [29,30] incorporates the string fusion phenomenon and is based on the parton model of strong interactions. The SFM framework is used to investigate the characteristics of the strongly intensive variable that characterizes correlations between the number of particles in two separated rapidity intervals in pp interactions at LHC energy [31]. Using various dynamics of the string interaction assumptions, correlations between multiplicities and average transverse momentum are accomplished in the percolating color strings picture [32,33]. A string percolation process in pp collisions was used to study the FB correlations [32] and observed an approximately constant FB correlation over a substantial range of rapidity window.

The correlations between mean transverse momentum and multiplicity of charged particles in pp and $p\bar{p}$ collisions at $\sqrt{s}$ from 17 GeV to 7 TeV are studied using a modified multi-Pomeron exchange model in which string collectivity has been included in an effective way [34]. In pp, pPb, and PbPb collisions at LHC energies it is explored using a dipole-based Monte Carlo string fusion model [35]. According to the color glass condensate model [36–38], long-range rapidity correlations continue throughout the development of the quark-gluon plasma that results from the collision. Using a model that regards strings as independent identical emitters, the FB charged-particle multiplicity correlations between windows spaced apart in rapidity and azimuth are investigated in Ref. [39]. The theoretical background of long-range correlations in heavy-ion collisions has been studied using a Monte Carlo method in Ref. [40].

The high multiplicity data of pp and pPb collisions at the LHC and dAu collisions at the RHIC show some collectivelike features resembling the heavy-ion collision [41–48]. The two-particle correlation studies in high-multiplicity pp/pPb collisions showed the heavy-ion signature: "the ridge," which triggered many theoretical discussions on the origin of it. Recent studies [49,50] show that the hydrodynamical modeling which remains successful in explaining many features of heavy-ion collisions is also found to be applicable in small collision systems. We discussed in our previous article [51] how the EPOS3 model [52] with hydrodynamical evolution of produced particles (referred to as "with hydro" in the rest of the text) successfully reproduced many features of small collision systems at the LHC energies [53]. Furthermore, we investigated the FB multiplicity and momentum correlations using the EPOS3 model by switching ON/OFF the hydrodynamical evolution of produced particles, which does not affect the final outcomes much. Studies using different models show that the FB correlation strength is found to be increasing with decreasing nuclear size upon the selected η-windows and with increasing collision energy for a fixed collision system [54,55]. It has also been proposed that instead of the contribution coming from particle production in the initial stages of collisions, the subsequent stage could modify the behavior of FB correlations, and hadron nucleus collision is expected to give more information on the whole scenario. Keeping this in mind, a comparative analysis of pp and pPb systems has been performed to improve our current understanding of FB phenomena. We have inspected FB multiplicity and momentum correlation in pp and pPb collisions at the center-of-mass energy $\sqrt{s} = 13$ TeV and $\sqrt{s_{\mathrm{NN}}} = 5.02$ TeV, respectively, using EPOS3 simulated with hydro events. In order to clarify the functions of each component of the model that contribute to the outcomes, we have further divided the model into core and corona approaches. The energy density of the strings in the core is sufficient to activate the hydrodynamically evolving QGP description. In the corona, hadron creation from nucleon-nucleon collisions is viewed as an independent phenomenon [52].

The rest of the paper is organized as follows: The definition of FB multiplicity and momentum correlation coefficients are introduced in Sec. II. Section III describes briefly the basic principles of the EPOS3 model and the sample size of generated events. The choice of EPOS3 simulated events and FB windows are illustrated in Sec. IV. In Sec. V, the dependence of FB correlation strength by

varying $\eta_{\rm gap}$, $\delta\eta$, $p_{T_{\rm min}}$, and different multiplicity classes are discussed in detail. More importantly, the behavior of the $\delta\eta$-weighted average of FB multiplicity and momentum correlation strengths as a function of the center-of-mass energy using EPOS3 simulated pp events are studied for the first time. Finally, conclusions are drawn in Sec. VI.

II. FORWARD-BACKWARD CHARGED-PARTICLE MULTIPLICITY AND MOMENTUM CORRELATION COEFFICIENT

Forward-backward correlations are measured between different observables in separated η-intervals, namely, n–n (the correlation between charged-particle multiplicities), p_T-p_T (the correlation between mean or summed transverse momenta of charged particles), and p_T–n (the correlation between mean or summed transverse momenta in one pseudorapidity interval and the multiplicity of charged particles in another pseudorapidity interval) [56]. Two η-intervals, one from the forward and another from the backward window, are symmetrically chosen around the collision center. The detailed window construction has already been shown and discussed in Ref. [51].

A linear relationship between average charged-particle multiplicity in the backward window ($\langle N_b\rangle_{N_f}$) and the charged-particle multiplicity in the forward window (N_f) has been reported and discussed in Refs. [12,13]:

$$\langle N_b\rangle_{N_f} = a + b_{\rm corr}({\rm mult})N_f. \tag{1}$$

Here, the FB multiplicity correlation strength is characterized by $b_{\rm corr}({\rm mult})$. Considering the linear relationship between ($\langle N_b\rangle_{N_f}$) and N_f, $b_{\rm corr}({\rm mult})$ can be determined using the following Pearson correlation coefficient:

$$b_{\rm corr}({\rm mult}) = \frac{\langle N_f N_b\rangle - \langle N_f\rangle\langle N_b\rangle}{\langle N_f^2\rangle - \langle N_f\rangle^2}. \tag{2}$$

The measurement of the FB multiplicity correlation coefficient $b_{\rm corr}({\rm mult})$ is defiled by the so-called "volume fluctuations," which arise due to the event-by-event fluctuations of the number of participating nucleons [57,58]. Hence, we have considered an intensive observable like the sum of the absolute transverse momentum of charged particles within the selected η-windows to reduce the contribution of volume fluctuations. Similar to the multiplicity correlation, we have estimated the FB momentum correlation coefficient $b_{\rm corr}(\Sigma p_T)$ using the following formula:

$$b_{\rm corr}(\Sigma p_T) = \frac{\langle \Sigma p_{T_f}\Sigma p_{T_b}\rangle - \langle \Sigma p_{T_f}\rangle\langle \Sigma p_{T_b}\rangle}{\langle (\Sigma p_{T_f})^2\rangle - \langle \Sigma p_{T_f}\rangle^2}. \tag{3}$$

Here, Σp_{T_f} (Σp_{T_b}) denotes the event-averaged transverse momenta of charged particles in the forward (backward) window.

An intuitive observable, the $\delta\eta$-weighted average of the FB multiplicity and momentum correlation strength, has been introduced for the first time and is defined as follows:

$$\langle b_{\rm corr}({\rm mult}/\Sigma p_T)\rangle_{\delta\eta} = \frac{\Sigma_i b_{\rm corr}({\rm mult}/\Sigma p_T)_i \delta\eta_i}{\Sigma_i \delta\eta_i}. \tag{4}$$

The behavior of such an observable has been studied as a function of the center-of-mass energy in pp collisions taking into account our earlier measurements in similar collision system [51].

III. EPOS3 MODEL

The EPOS3 model [52] is based on Gribov-Regge multiple scattering theory. In this approach an individual scattering is labeled as a "Pomeron." A Pomeron creates a parton ladder which may be considered as a longitudinal flux tube carrying the transverse momentum from the initial hard scatterings [59]. In a collision, many elementary parton-parton hard scatterings form a large number of flux tubes that expand and are fragmented into string segments. Higher string density forms the so-called "core" which undergoes a three-dimensional $(3{\rm D})+1$ viscous hydrodynamical evolution expecting no jet parton escapes and hadronizes via the usual Cooper-Frye formalism at a "hadronization temperature" $T_{\rm H}$. Another part of the lower string density forms the so-called "corona" where we can expect the escape of jet partons. Such string segments having high transverse momentum that are close to the surface leave the bulk matter and hadronize (including jet hadrons) via the Schwinger mechanism. The phase transition from parton to hadron follows a realistic equation of state which is compatible with the lattice gauge results with subsequent hadronic cascade using the UrQMD model [60].

Using the EPOS3 model, we have generated 3×10^6 minimum-bias pp events at $\sqrt{s}=13$ TeV and pPb events at $\sqrt{s_{\rm NN}}=5.02$ TeV. On top of the minimum-bias analysis, a more differential approach has been introduced by taking particles coming from either the core or corona, and we have varied certain model parameters in order to achieve it. We have measured the FB multiplicity and momentum correlations for the EPOS3 generated events with all charged particles and particles from the core and corona.

To validate the generated event samples of different center-of-mass energies, we have compared minimum-bias EPOS3 simulated events with ALICE data [61–63]. Figure 1 shows that the invariant yields of charged particles as a function of p_T as measured by the ALICE experiment in pp collisions at $\sqrt{s}=13$ TeV (top) and in pPb collisions at $\sqrt{s_{\rm NN}}=5.02$ TeV (bottom) have been successfully reproduced by the EPOS3 simulated events at the chosen energies. Average pseudorapidity density and pseudorapidity density of charged particles has been plotted in Fig. 2 for EPOS3 simulated pp events at $\sqrt{s}=13$ TeV

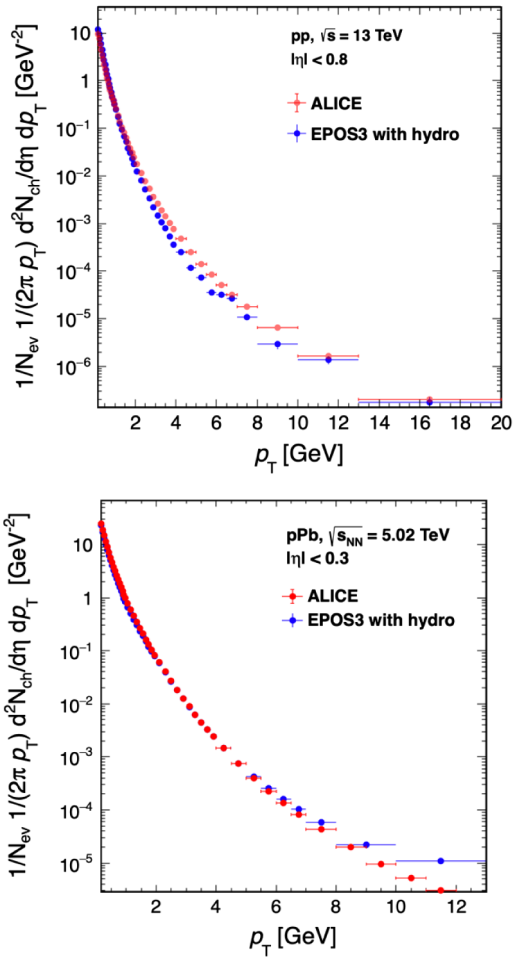

FIG. 1. Charged-particle invariant yields as a function of p_T in pp collisions at $\sqrt{s} = 13$ TeV (top) and in pPb collisions at $\sqrt{s_{\rm NN}} = 5.02$ TeV (bottom) compared to ALICE data [61,62].

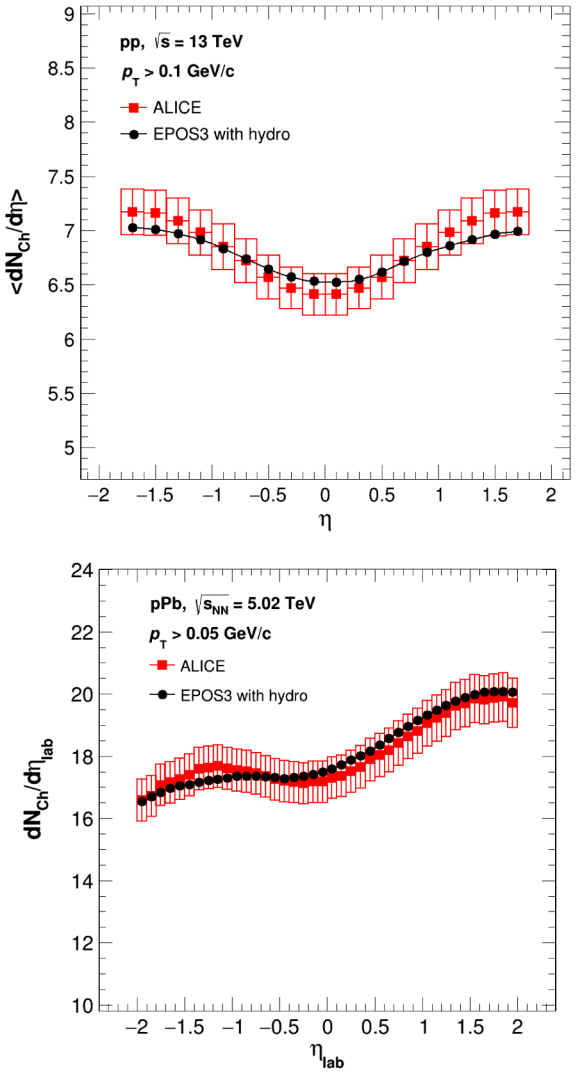

FIG. 2. Average pseudorapidity density of charged particles in pp collisions at $\sqrt{s} = 13$ TeV (top) and pPb collisions at $\sqrt{s_{\rm NN}} = 5.02$ TeV (bottom) compared to ALICE data [61,63].

(top) and pPb events at $\sqrt{s_{\rm NN}} = 5.02$ TeV (bottom), respectively. The compared results reflect that the EPOS3 simulated events agree well with the experimental measurements in the chosen kinematic intervals [61,63].

IV. EVENTS AND FB WINDOW SELECTION

Events are selected with a minimum of two charged particles in the chosen kinematic interval. All analyses of the pp and pPb events have been carried out following ALICE [24] and ATLAS [23] kinematics. By ALICE kinematics, we mean the cuts on the kinematic variables p_T and η as $0.3 < p_T < 1.5$ GeV/c and $|\eta| < 0.8$, respectively. Similarly, for the ATLAS kinematics we use $p_T > 0.1$ GeV/c and $|\eta| < 2.5$. The only caveat is that those cuts were used for lower center-of-mass energies for pp collisions by the ALICE and ATLAS Collaborations.

V. RESULTS AND DISCUSSION

We have calculated and plotted in Fig. 3 the average backward multiplicity ($\langle N_b \rangle_{N_f}$) for each fixed value of forward multiplicity N_f for window width $\delta\eta = 0.6$ and $\eta_{\rm gap} = 0.4$ for EPOS3 simulated pp events at $\sqrt{s} = 13$ TeV (left panel) and pPb events at $\sqrt{s_{\rm NN}} = 5.02$ TeV (right panel). From the scatter plots we can see a linear relationship between $\langle N_b \rangle_{N_f}$ and N_f. A linear fit has been displayed by the red lines in both panels. The slope of these lines actually quantifies the correlation strength between multiplicities in the FB windows. We have therefore applied the Pearson correlation coefficient formula described in Eq. (2) to compute FB multiplicity correlation strengths. To eliminate the incorporated volume fluctuations in the FB multiplicity correlation, we have evaluated the FB momentum correlation coefficient $b_{\rm corr}(\Sigma p_T)$ using Eq. (3) for the EPOS3 simulated pp events at $\sqrt{s} = 13$ TeV and pPb events at $\sqrt{s_{\rm NN}} = 5.02$ TeV.

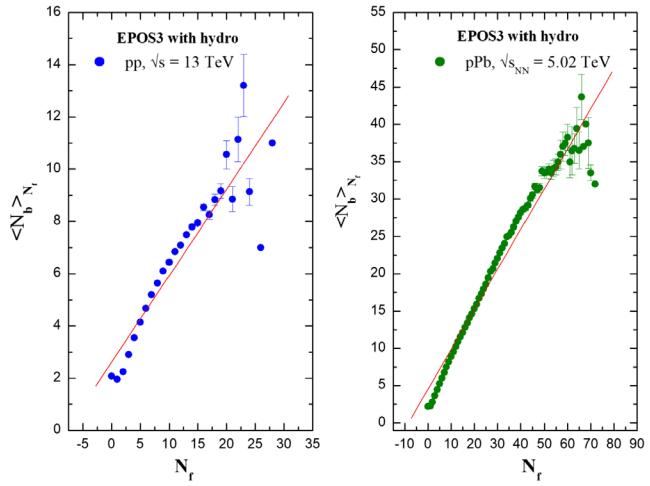

FIG. 3. Variation of $\langle N_b \rangle_{N_f}$ with N_f for FB window width $\delta\eta = 0.6$ and $\eta_{\rm gap} = 0.4$ for EPOS3 generated pp events at $\sqrt{s} = 13$ TeV (left panel) and pPb events (right panel) at $\sqrt{s_{\rm NN}} = 5.02$ TeV. A linear fit has been performed (red line) for both systems.

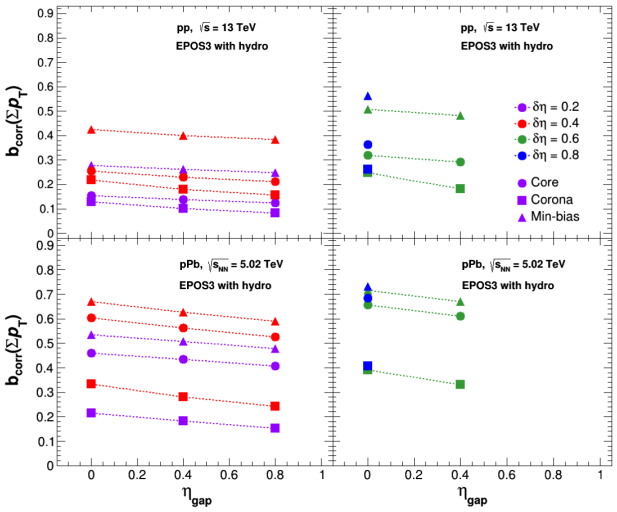

FIG. 5. Forward-backward summed-p_T correlation as a function of $\eta_{\rm gap}$ for four window widths $\delta\eta = 0.2$, 0.4, 0.6, and 0.8 for EPOS3 generated all charged particles and particles from the core and corona in pp and pPb collisions at $\sqrt{s} = 13$ TeV (top panel) and $\sqrt{s_{\rm NN}} = 5.02$ TeV (bottom panel), respectively.

A. Dependence on the gap between FB windows ($\eta_{\rm gap}$)

The variation of FB multiplicity and momentum correlation coefficients with $\eta_{\rm gap}$ for four different window widths ($\delta\eta = 0.2$, 0.4, 0.6, and 0.8) are shown in Figs. 4 and 5, respectively, for EPOS3 simulated all charged particles, core-only and corona-only particles in pp collisions at $\sqrt{s} = 13$ TeV (top panel), and pPb collisions at $\sqrt{s_{\rm NN}} = 5.02$ TeV (bottom panel). We have compared all three cases for window widths $\delta\eta = 0.2$ and 0.4 (left panel) and $\delta\eta = 0.6$ and 0.8 (right panel) for both pp and pPb events. We observed that for a fixed window width, the FB correlation strengths decrease slowly with increasing $\eta_{\rm gap}$ and increase with increasing $\delta\eta$ at a fixed $\eta_{\rm gap}$, which resemble the trend at lower center-of-mass energies in pp collisions as described in our earlier study [51].

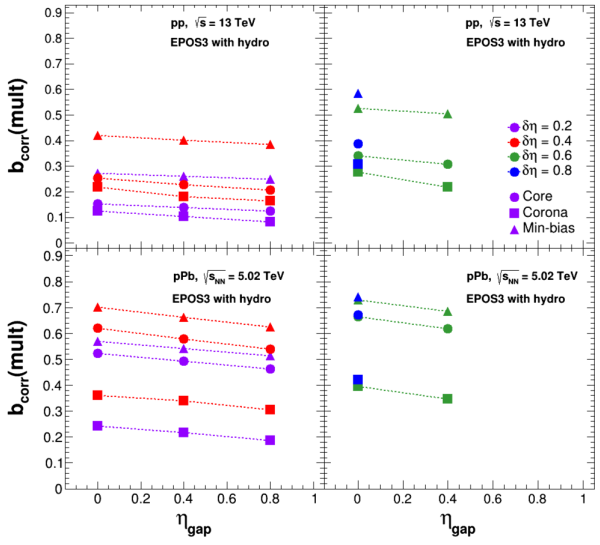

FIG. 4. FB multiplicity correlation strength $b_{\rm corr}({\rm mult})$ as a function of $\eta_{\rm gap}$ for $\delta\eta = 0.2$, 0.4, 0.6, and 0.8 for EPOS3 generated all charged particles and particles from the core and corona in pp collisions at $\sqrt{s} = 13$ TeV (top panel) and pPb collisions (bottom panel) at $\sqrt{s_{\rm NN}} = 5.02$ TeV.

Quantitatively, we found that the correlation strengths are larger for pPb collisions than for pp collisions for all chosen $\eta_{\rm gap}$ and $\delta\eta$ combinations. The asymmetric nature of pPb collisions where the proton collides with a nucleus having a larger number of sources compared to pp collisions, results in a larger initial-state parton density in the lead nucleus compared to the proton. Such asymmetric collisions could have larger fluctuations in the final state which may contribute to stronger forward-backward correlation strength in pPb collisions with respect to pp collisions.

Interestingly, we have noticed that for pPb events the correlation strengths decrease faster with increasing $\eta_{\rm gap}$ as compared to pp events. The SRC component depends strongly on the collision system, and it is asymmetric between the forward and backward windows in pPb collisions, while the LRC component is nearly symmetric in all collision systems [9]. Thus, the faster dilution of the SRC component at large $\eta_{\rm gap}$ between the forward and backward regions could be the reason behind the faster decrease of correlation strength in asymmetric pPb collisions with respect to symmetric pp collisions.

The dominance of correlation strength due to core-only particles is clearly visible over corona-only particles. Since the particles from the corona are mostly dominated by jets or minijet partons, the paucity of the LRC component results in smaller correlation strength for

particles from the corona over the core at large $\eta_{\rm gap}$ for both collision systems.

B. Dependence on the width of FB windows ($\delta\eta$)

The $\delta\eta$ dependence of FB multiplicity and momentum correlation coefficients for contiguous ($\eta_{\rm gap} = 0$) symmetrical windows with respect to the collision center are shown in Figs. 6 and 7 for $\sqrt{s} = 13$ TeV in pp collisions and $\sqrt{s_{\rm NN}} = 5.02$ TeV in pPb collisions using EPOS3 simulated with hydro events. We have studied and presented the multiplicity and momentum correlation coefficients for the EPOS3 generated event samples with all charged particles and particles from the core and corona. We observed that the core-only and corona-only cases underestimate both the correlation strengths for minimum-bias event sample. The correlation coefficients increase nonlinearly with $\delta\eta$ for both pp and pPb events though the values are higher in the case of pPb events, which may be due to fact as described in Sec. V A. The results are found to be similar to our earlier measurements qualitatively [51], featuring the dominance of a SRC component for the nonlinear growth of the FB correlation strengths. As discussed and explained in Sec. V A, here also we have found that the correlation strengths with respect to $\delta\eta$ are larger for the core-only particles than they are for the corona-only particles.

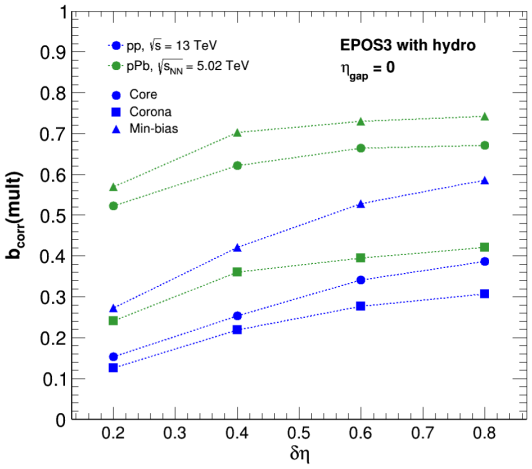

FIG. 6. FB multiplicity correlation strength $b_{\rm corr}({\rm mult})$ as a function of $\delta\eta$ for $\eta_{\rm gap} = 0$ using EPOS3 generated pp and pPb events at $\sqrt{s} = 13$ TeV and $\sqrt{s_{\rm NN}} = 5.02$ TeV, respectively, for all charged particles and particles from the core and corona.

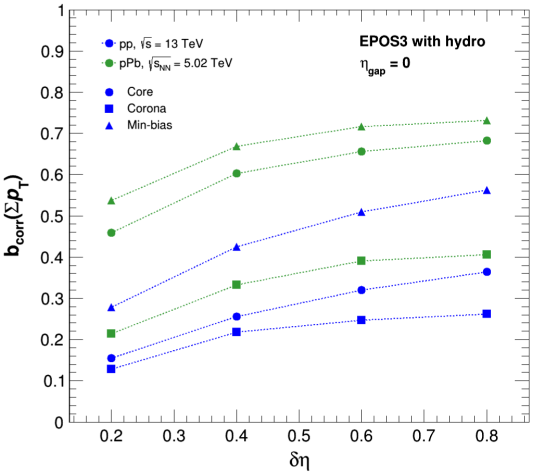

FIG. 7. Contributions of $b_{\rm corr}(\Sigma p_T)$ on $\delta\eta$ for $\eta_{\rm gap} = 0$ for EPOS3 generated pp and pPb events.

C. Dependence on collision energy ($\sqrt{s}$)

We have examined the behavior of the $\delta\eta$-weighted average of FB multiplicity and momentum correlation strengths as a function of the center-of-mass energy using EPOS3 simulated pp event samples. Such an unconventional measurement is still not available experimentally. Hence, to compare our findings in a systematic way, we have evaluated the $\delta\eta$-weighted average for the available experimental $b_{\rm corr}({\rm mult})$ and $b_{\rm corr}(\Sigma p_T)$ values for the ALICE [24] and ATLAS [23] data. Figures 8 and 9 show the $\delta\eta$-weighted average of FB multiplicity and momentum correlation as a function of the center-of-mass energy following ALICE and ATLAS kinematics.

In the left panel of Figs. 8 and 9, we observed that initially the $\langle b_{\rm corr}({\rm mult})\rangle_{\delta\eta}$ and $\langle b_{\rm corr}(\Sigma p_T)\rangle_{\delta\eta}$ values increase rapidly with increasing $\sqrt{s}$ up to 2.76 TeV, then they grow moderately up to $\sqrt{s} = 7$ TeV for both EPOS3 simulated events and experimental data. For comparison, we have incorporated the results from other available theoretical models which also show a similar trend for the $\delta\eta$-weighted average of FB correlations [28,39].

It is also very interesting to find that for EPOS3 simulated events, the $\delta\eta$-weighted average of FB

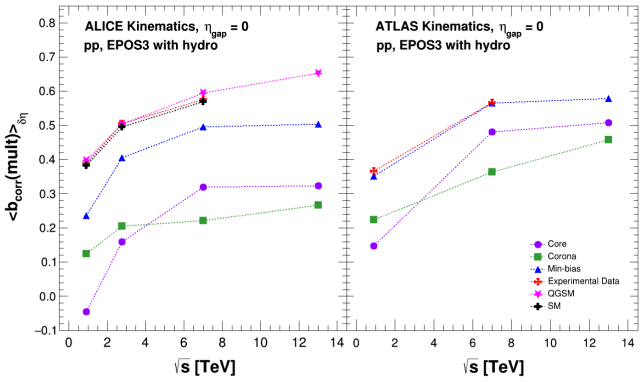

FIG. 8. Comparison of $\delta\eta$-weighted average FB multiplicity correlations ($\langle b_{\rm corr}({\rm mult})\rangle_{\delta\eta}$) as a function of $\sqrt{s}$ for the EPOS3 simulated pp events (all charged particles, core, and corona) with derived ALICE (left) and ATLAS (right) data, and theoretical models (left).

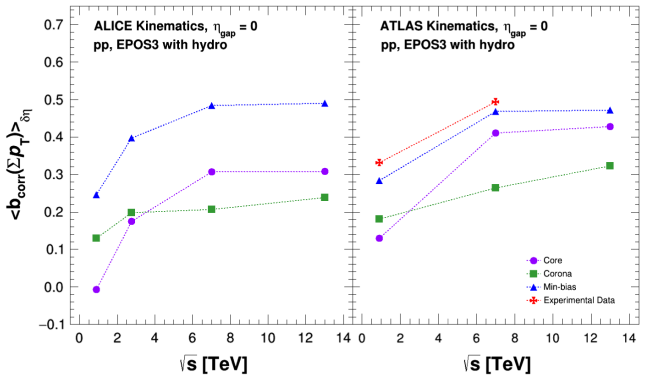

FIG. 9. Comparison of $\delta\eta$-weighted average FB summed-p_T correlations ($\langle b_{\rm corr}(\Sigma p_T)\rangle_{\delta\eta}$) as a function of $\sqrt{s}$ for EPOS3 simulated pp events (all charged particles, core, and corona) following ALICE kinematics (left) and with derived ATLAS (right) data.

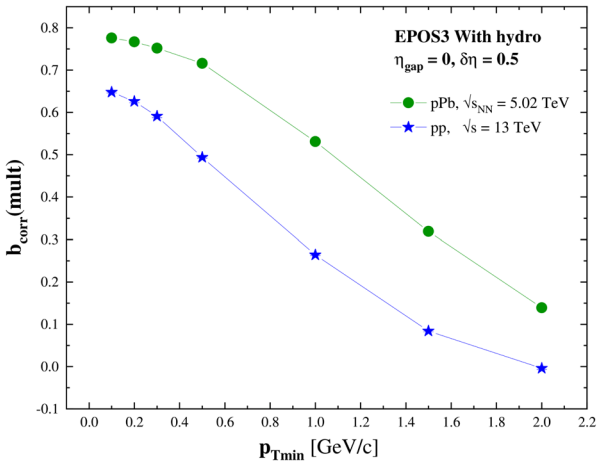

FIG. 10. Forward-backward multiplicity correlations as a function of $p_{T_{\rm min}}$ for window width $\delta\eta = 0.5$ for EPOS3 simulated pp and pPb events.

correlation strengths as a function of $\sqrt{s}$ lean toward saturation approximately beyond $\sqrt{s} = 7$ TeV, where there is no available experimental data for such a measurement. The results from the QGSM model though do not show such a strong saturation effect at higher energy.

To gain a more nuanced understanding of the fascinating behavior observed in the $\delta\eta$-weighted average of FB correlation strengths, we computed this metric separately for the particles coming either from the core or corona. We have found that the observed saturation at higher center-of-mass energy is predominantly due to the saturation for the core-only particles, whereas the corona-only particles show an increasing trend. In the EPOS3 model, the corona is dominated by the high-p_T particles, whereas the core contains particles which undergo $3+1$D hydro mimicking the formation of a QGP-like medium [64].

The exchange of multiple Pomerons between colliding particles [65] in a collision remains the primary source of fluctuations producing multiple particles in a correlated way. The multiplicity of produced particles and their transverse momentum is thus very much influenced by the initial conditions of a collision, and in particular, they are much more apparent in small collision systems like pp or pA where final-state effects are less. In the CGC framework [66,67], it has been argued that at small $x \sim p_T/\sqrt{s}$, gluon density first grows and then gets saturated with an increase in energy which results in a moderate increase in charge particle multiplicity density in pp or pA collisions as the beam energy increases [68]. Since an observable like $b_{\rm corr}$ is an extensive quantity, it might show such a saturation effect mainly because fluctuations associated with the number of sources get saturated [65]. Henceforth, the EPOS3-model-based FB correlation analysis at higher center-of-mass energy encourages further experimental study.

D. Dependence on the minimum transverse momentum ($p_{T_{\rm min}}$)

The variation of FB multiplicity and momentum correlations with the minimum transverse momentum of charged particles ($p_{T_{\rm min}}$) are shown in Figs. 10 and 11 for the EPOS3 generated model with both hydro pp events at $\sqrt{s} =$ 13 TeV and pPb events at $\sqrt{s_{\rm NN}} = 5.02$ TeV following ATLAS kinematics [23]. We calculated the values of $b_{\rm corr}$ at seven different levels of minimum transverse momentum ($p_{T_{\rm min}}$), specifically at $p_{T_{\rm min}} = 0.1$, 0.2, 0.3, 0.5, 1.0, 1.5, and 2.0 GeV. These calculations were performed for symmetric FB windows without any separation. The multiplicity and momentum correlation strengths decrease rapidly with the increase of $p_{T_{\rm min}}$ values for both pp and pPb events confirming a similar trend at lower center-of-mass energies [51]. With the increase of $p_{T_{\rm min}}$,

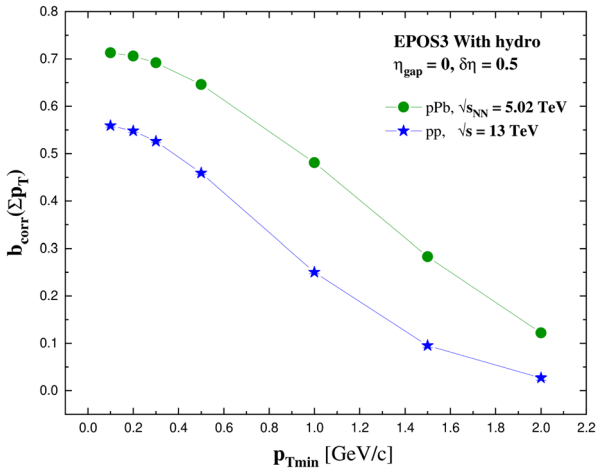

FIG. 11. Forward-backward summed-p_T correlation as a function of $p_{T_{\rm min}}$ for window width $\delta\eta = 0.5$ for EPOS3 generated pp and pPb events.

the domination of the LRC component decreases resulting in weaker FB multiplicity correlation strength, suggesting the transition from the soft process to the hard processes with increasing transverse momentum of the produced particles. As discussed in Sec. V A, here also the correlation strengths are found to be greater for pPb collisions than for pp collisions.

E. Multiplicity-dependent $b_{\mathrm{corr}}(\Sigma p_T)$

In addition to the study using minimum-bias EPOS3 events, we have exploited a multiplicity-dependent summed-p_T FB correlations study as well. Figures 12 and 13 show the FB momentum correlation as a function of η_{gap} for $\delta\eta = 0.5$ in three multiplicity ranges estimated following ATLAS kinematics [23] using EPOS3 simulated pp events at $\sqrt{s} = 13$ TeV and pPb events at

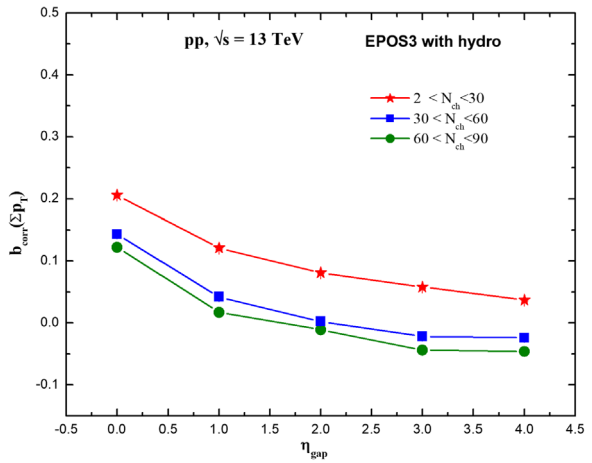

FIG. 12. Forward-backward summed-p_T correlations as a function of η_{gap} for window width $\delta\eta = 0.5$ in different multiplicity ranges for EPOS3 simulated pp events at $\sqrt{s} = 13$ TeV.

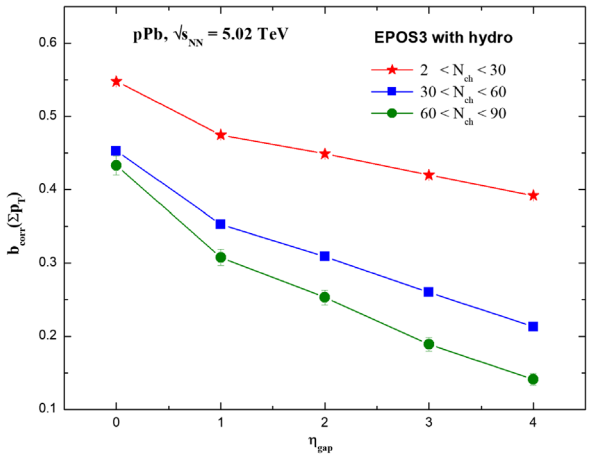

FIG. 13. Forward-backward summed-p_T correlations as a function of η_{gap} for window width $\delta\eta = 0.5$ in different multiplicity ranges for EPOS3 simulated pPb events at $\sqrt{s_{\mathrm{NN}}} = 5.02$ TeV.

$\sqrt{s_{\mathrm{NN}}} = 5.02$ TeV. The red, blue, and green points correspond to nonoverlapping multiplicity regions: low-multiplicity ($2 < \mathrm{N_{ch}} < 30$), midmultiplicity ($30 < \mathrm{N_{ch}} < 60$), and high-multiplicity ($60 < \mathrm{N_{ch}} < 90$) regions, respectively. We have kept the multiplicity ranges the same for both pp and pPb events for better understanding. We can see a similar decrease of the correlation strength with increasing η_{gap} and for a fixed η_{gap} value, $b_{\mathrm{corr}}(\Sigma p_T)$ also decreases with increasing multiplicity, which may be due to the fact that the fusion of strings into the core in high-multiplicity EPOS3 events lowers the FB correlation strength [51].

VI. SUMMARY AND CONCLUSIONS

We have performed a rigorous study of FB multiplicity and momentum correlation in pp and pPb collisions at center-of-mass energies $\sqrt{s} = 13$ TeV and $\sqrt{s_{\mathrm{NN}}} = 5.02$ TeV, respectively, at the LHC using EPOS3 simulated events with all charged particles and particles from the core and corona. We have investigated the behavior of the FB correlation strengths on the gap between two pseudorapidity windows (η_{gap}), window width ($\delta\eta$), minimum transverse momentum ($p_{T_{\mathrm{min}}}$), and different multiplicity classes. Many LHC findings confirm a strong analogy between the small collision systems pp and pPb, particularly in terms of particle correlations and fluctuations [42,43,69]. We have also noticed here that general trends of both FB correlation strengths are similar in case of EPOS3 simulated pp and pPb events irrespective of energy difference. We have found the following results:

(i) The linear relationship between $\langle N_b \rangle_{N_f}$ and N_f is verified for both EPOS3 generated pp and pPb events and is more steeper for the pPb events than it is for the pp events.

(ii) Our model-based study fairly describes two general features of both FB correlation coefficients in two different collision systems (pp and pPb) in that it decreases slowly with the increase of gap between two selected η-windows irrespective of the window widths and increases nonlinearly with the window width for a fixed separation between η-windows.

(iii) A rapid decrease in the values of both $b_{\mathrm{corr}}(\mathrm{mult})$ and $b_{\mathrm{corr}}(\sum p_T)$ with a small increase of minimum transverse momentum $p_{T_{\mathrm{min}}}$ has been observed for both pp and pPb events.

(iv) Multiplicity-dependent summed-p_T correlation study also reveals that with the increase of multiplicity, the value of $b_{\mathrm{corr}}(\sum p_T)$ decreases at a fixed η_{gap} for both pp and pPb events.

All these facts resemble our previous assessment of FB correlations in pp collisions at three comparatively lower center-of-mass energies $\sqrt{s} = 0.9$, 2.76, and 7 TeV [51]. The observed larger FB multiplicity and momentum

correlation strength in pPb collisions with respect to pp collisions could be due to the fact that the initial asymmetry of the pPb collisions and the large system size with respect to the pp collisions may enhance the event-by-event fluctuations, which in turn may increase the FB correlation.

The most interesting result from our present study is the behavior of the $\delta\eta$-weighted average of the FB multiplicity and momentum correlation strengths as a function of the center-of-mass energy ($\sqrt{s} = 0.9$, 2.76, 7, and 13 TeV) using EPOS3 simulated pp events. The increase of both the correlation strengths [$b_{\mathrm{corr}}(\mathrm{mult})$ and $b_{\mathrm{corr}}(\Sigma p_T)$] with $\sqrt{s}$ is clearly visible, and interestingly, we have observed that it tends to saturate at very high energy. We have incorporated different theoretical model studies to compare our results, and the correlation strengths have been found to follow a similar trend as the EPOS3 simulated events. To investigate the possible reason behind such an interesting observation, we have calculated the correlation strengths for the EPOS3 generated events with all charged particles and particles from the core and corona. We have found that for the particles from the corona, the $\delta\eta$-weighted average of FB correlations does not show any saturation trend, whereas the particles from the core perfectly exhibit the trend. We have inferred that it may be due to the dominance of the gluon-saturation effect at such higher center-of-mass energies.

Our analyses have uncovered the fact that the FB multiplicity and momentum correlation as a function of η_{gap}, $\delta\eta$, $p_{T_{\mathrm{min}}}$, and different multiplicity classes in EPOS3 simulated pPb events qualitatively resemble the outcome of EPOS3 simulated pp events, though the values of the correlation coefficients are higher for pPb events than those for the pp events. Overall, we may conclude that the systematic study of FB correlations in different dimensions using the hybrid Monte Carlo model EPOS3 [52] adds more valuable information to understand the existing experimental results as well as encourages more experimental measurements at higher center-of-mass energies and in different collision systems.

ACKNOWLEDGMENTS

The authors thank Dr. Klaus Warner for providing us with the EPOS3 model. The authors thank the members of the grid computing team of VECC and cluster computing team of the Department of Physics, Jadavpur University for providing an uninterrupted facility for event generation and analyses. We also gratefully acknowledge the financial help from the DST-GOI under the scheme "Mega facilities in basic science research" [Sanction Order No. SR/MF/PS-02/2021-Jadavpur (E-37128) dated December 31, 2021]. J. M. acknowledges DST-INDIA for providing a fellowship under the INSPIRE scheme.

[1] E. Shuryak, Rev. Mod. Phys. **89**, 035001 (2017).
[2] P. Braun-Munzinger, V. Koch, T. Schaefer, and J. Stachel, Phys. Rep. **621**, 76 (2016).
[3] K. Fukushima and T. Hatsuda, Rep. Prog. Phys. **74**, 014001 (2011).
[4] C. Gale, S. Jeon, and B. Schenke, Int. J. Mod. Phys. A **28**, 1340011 (2013).
[5] U. Heinz and R. Snellings, Annu. Rev. Nucl. Part. Sci. **63**, 123 (2013).
[6] B. Schenke, S. Jeon, and C. Gale, Phys. Rev. Lett. **106**, 042301 (2011).
[7] B. Schenke, S. Jeon, and C. Gale, Phys. Rev. C **85**, 024901 (2012).
[8] G. Aad *et al.* (ATLAS Collaboration), Phys. Rev. C **86**, 014907 (2012).
[9] M. Aaboud *et al.* (ATLAS Collaboration), Phys. Rev. C **95**, 064914 (2017).
[10] A. Capella and A. Krzywicki, Phys. Rev. D **18**, 4120 (1978).
[11] K. Alpgard *et al.* (UA5 Collaboration), Phys. Lett. **123B**, 361 (1983).
[12] G. J. Alner *et al.* (UA5 Collaboration), Phys. Rep. **154**, 247 (1987).
[13] R. E. Ansorge *et al.* (UA5 Collaboration), Z. Phys. C **37**, 191 (1988).
[14] L. V. Bravina *et al.*, Sov. J. Nucl. Phys. **50**, 245 (1989), https://inspirehep.net/literature/287553.
[15] V. V. Aivazyan *et al.* (NA22 Collaboration), Z. Phys. C **42**, 533 (1989).
[16] T. Alexopoulos *et al.* (E735 Collaboration), Phys. Lett. B **353**, 155 (1995).
[17] M. Derrick *et al.* (HRS Collaboration), Phys. Rev. D **34**, 3304 (1986).
[18] W. Braunschweig *et al.* (TASSO Collaboration), Z. Phys. C **45**, 193 (1989).
[19] R. Akers *et al.* (OPAL Collaboration), Phys. Lett. B **320**, 417 (1994).
[20] A. Giovannini and R. Ugoccioni, Phys. Rev. D **66**, 034001 (2002).
[21] B. B. Back *et al.* (PHOBOS Collaboration), Phys. Rev. C **74**, 011901 (2006).
[22] B. I. Abelev *et al.* (STAR Collaboration), Phys. Rev. Lett. **103**, 172301 (2009).
[23] G. Aad *et al.* (ATLAS Collaboration), J. High Energy Phys. 07 (2012) 019.
[24] J. Adam *et al.* (ALICE Collaboration), J. High Energy Phys. 05 (2015) 097.
[25] A. Capella, U. Sukhatme, C.-I. Tan, and J. T. T. Van, Phys. Rep. **236**, 225 (1994).

[26] A. Capella, U. Sukhatme, C.-I. Tan, and J. T. T. Van, Phys. Rep. **236**, 225 (1994).
[27] A. B. Kaidalov, Phys. Lett. **116B**, 459 (1982); Phys. At. Nucl. **66**, 1994 (2003).
[28] L. V. Bravina, J. Bleibel, and E. E. Zabrodin, Phys. Lett. B **787**, 146 (2018).
[29] N. S. Amelin, M. A. Braun, and C. Pajares, Phys. Lett. B **306**, 312 (1993); Z. Phys. C **63**, 507 (1994); N. S. Amelin, N. Armesto, M. A. Braun, E. G. Ferreiro, and C. Pajares, Phys. Rev. Lett. **73**, 2813 (1994).
[30] M. A. Braun and C. Pajares, Nucl. Phys. **B390**, 542 (1993).
[31] V. V. Vechernin and S. N. Belokurova, J. Phys. Conf. Ser. **1690**, 012088 (2020); E. Andronov and V. V. Vechernin, Eur. Phys. J. A **55**, 14 (2019).
[32] P. Brogueira, J. Dias de Deus, and C. Pajares, Phys. Lett. B **675**, 308 (2009).
[33] M. A. Braun, R. S. Kolevatov, C. Pajares, and V. V. Vechernin, Eur. Phys. J. C **32**, 535 (2004).
[34] E. O. Bodnya, V. N. Kovalenko, A. M. Puchkov, and G. A. Feofilov, AIP Conf. Proc. **1606**, 273 (2014).
[35] V. N. Kovalenko, Phys. Part. Nucl. **48**, 945 (2017).
[36] L. McLerran, Nucl. Phys. **A699**, 73 (2002).
[37] N. Armesto, L. McLerran, and C. Pajares, Nucl. Phys. **A781**, 201 (2007).
[38] T. Lappi and L. McLerran, Nucl. Phys. **A832**, 330 (2010).
[39] V. Vechernin, Nucl. Phys. **A939**, 21 (2015); Proc. Sci. QFTHEP2013 (**2013**) 055.
[40] V. V. Vechernin and R. S. Kolevatov, Phys. At. Nucl. **70**, 1797 (2007); **70**, 1809 (2007).
[41] V. Khachatryan *et al.* (CMS Collaboration), Phys. Rev. Lett. **116**, 172302 (2016).
[42] V. Khachatryan *et al.* (CMS Collaboration), Phys. Lett. B **765**, 193 (2017).
[43] B. Abelev *et al.* (ALICE Collaboration), Phys. Lett. B **719**, 29 (2013).
[44] S. Chatrchyan *et al.* (CMS Collaboration), Phys. Lett. B **718**, 795 (2013).
[45] G. Aad *et al.* (ATLAS Collaboration), Phys. Rev. Lett. **110**, 182302 (2013).
[46] A. Adare *et al.* (PHENIX Collaboration), Phys. Rev. Lett. **114**, 192301 (2015).
[47] V. Khachatryan *et al.* (CMS Collaboration), J. High Energy Phys. 09 (2010) 091.
[48] G. Aad *et al.* (ATLAS Collaboration), Phys. Rev. Lett. **116**, 172301 (2016).
[49] K. Werner, I. Karpenko, and T. Pierog, Phys. Rev. Lett. **106**, 122004 (2011).
[50] P. Bozek, Phys. Rev. C **85**, 014911 (2012).
[51] M. Mondal, J. Mondal, S. Kar, A. Deb, and P. Ghosh, Phys. Rev. D **102**, 014033 (2020).
[52] K. Werner, B. Guiot, Iu. Karpenko, and T. Pierog, Phys. Rev. C **89**, 064903 (2014).
[53] S. Kar, S. Choudhury, S. Sadhu, and P. Ghosh, J. Phys. G **45**, 125103 (2018).
[54] Yi-An Li, Dong-Fang Wang, Song Zhang, and Yu-Gang Ma, Phys. Rev. C **104**, 044906 (2021).
[55] N. Armesto, M. A. Braun, and C. Pajares, Phys. Rev. C **75**, 054902 (2007).
[56] B. Alessandro *et al.* (ALICE Collaboration), J. Phys. G **32**, 1295 (2006).
[57] V. P. Konchakovski, H. Hauer, G. Torrieri, M. I. Gorenstein, and E. L. Bratkovskaya, Phys. Rev. C **79**, 034910 (2009).
[58] A. Bzdak, Phys. Rev. C **80**, 024906 (2009).
[59] H. J. Drescher, M. Hladik, S. Ostapchenko, T. Pierog, and K. Werner, Phys. Rep. **350**, 93 (2001).
[60] M. Bleicher *et al.*, J. Phys. G **25**, 1859 (1999); H. Petersen, J. Steinheimer, G. Burau, M. Bleicher, and H. Stöcker, Phys. Rev. C **78**, 044901 (2008).
[61] J. Adam *et al.* (ALICE Collaboration), Phys. Lett. B **753**, 319 (2016).
[62] B. Abelev *et al.* (ALICE Collaboration), Eur. Phys. J. C **74**, 3054 (2014).
[63] B. Abelev *et al.* (ALICE Collaboration), Phys. Rev. Lett. **110**, 032301 (2013).
[64] J. Aichelin and K. Werner, J. Phys. G **37**, 094006 (2010).
[65] V. Kovalenko, G. Feofilov, A. Puchkov, and F. Valiev, Universe **8**, 246 (2022).
[66] Larry McLerran, arXiv:0804.1736v1.
[67] F. Gelis, J. Phys. G **34**, S421 (2007).
[68] J. Adam *et al.* (ALICE Collaboration), Phys. Rev. Lett. **116**, 222302 (2016).
[69] V. Khachatryan *et al.* (CMS Collaboration), Phys. Lett. B **742**, 200 (2015).